MODELLING UNCERTAINTY FOR FLASH FLOODS IN COASTAL PLAINS USING ADJOINT METHODS

Hossam Elhanafy *, Graham J.M. Copeland **.

ABSTRACT:

This paper shows the application of adjoint sensitivity analysis to flash flood wave propagation in a river channel. The adjoint sensitivity analysis is used to assess flood hazard in a coastal area caused by river discharge. The numerical model determines the sensitivities of predicted water levels to uncertainties in key controls such as inflow hydrograph, channel topography, frictional resistance and infiltration rate. Sensitivities are calculated using the adjoint equations and are specified in terms of water levels being greater than certain safe threshold levels along the channel. The flood propagation model is based on the St. Venant equations while the propagation of sensitivity information is based on the corresponding adjoint equations. This analysis is achieved using a numerical model that integrates The St. Venant equations forward in time using a staggered finite difference scheme. An enhanced method of characteristics at the downstream boundary provides open boundary conditions and overcomes the problem of reflections from the boundaries. Then, the adjoint model is integrated backwards in time to trace the sensitivity information back through the model domain towards the inflow control boundary. The adjoint model has been verified by means of an identical twin experiment. As a study case, the method is applied to the main stream of a certain watershed at the north coast of Egypt and the location of the specified safe water levels are chosen to be near a culvert beneath the international coastal highway which extends from Egypt to Libya.

KEYWORDS

Data assimilation analysis; Open channel flow; Adjoint sensitivity analysis; Numerical models; Flash floods.

* PhD student, Civil Engineering Department, Strathclyde University, Scotland, U.K.
Email: hossam.el-hanafy@strath.ac.uk
** Reader, Civil Engineering Department, Strathclyde University, Scotland, U.K.
Email: g.m.copeland@strath.ac.uk

INTRODUCTION

The quality of flood predictions by numerical models depends on the accuracy of the inflow hydrograph, other control variables such as bed roughness, bed slope, and infiltration rate. However, each of these has its own effect on the predicted flood level. This research examines what effect uncertainties in the values of these controls have on the flood prediction. That is, we find out how the overall sensitivity of the flood level prediction could be apportioned to the individual sensitivity of each of the control variables. This could be done at significant computational expense using multiple runs and ensemble techniques. However, the adjoint method presented here determines these sensitivities analytically in one run of the model. Flood wave propagation models are often used when planning flood management strategies (Moussa et al. 1999) and it is important to consider what control actions could mitigate flood impact. Such controls could be hydraulic structures such as gates, locks, and weirs (Sanders and Katapodes, 1998), or the diversion of water into canals and floodplain storage facilities (Sanders and Katapodes, 2000). However, the term 'control' is also used for a user-defined value that determines the result of a model forecast, rather than offering an actual engineering control. This paper presents an analysis of how a model prediction of flood water level at a certain location is sensitive to variations in some of these control values. These sensitivities can be used to select the most appropriate location and rate of abstraction for flood control (Ding and Wang, 2006) to optimize water abstraction for irrigation (Sanders and Katapodes, 2000) or to identify Manning's roughness coefficient (Ding et al. 2004). The sensitivities can also be used for data assimilation (Cacuci, 2003) and (Navon and Zou 1991) , for ranking the parameters according to their effect on the flood level (Elhanafy and Copeland, 2007b). and to quantify the uncertainty in the predicted flood level to uncertainties in control variables as shown in this paper. The adjoint sensitivity analysis has been implemented through the development of two numerical models; a forward model, based on the Saint Venant equations (SVE[s]) used to simulate the propagation of the flood wave, and an adjoint model used to evaluate the time-dependent sensitivities with respect to a variety of control variables under different flow conditions. The adjoint method requires that the forward problem and its associated adjoint problem are solved sequentially. Sensitivity expressions which are functions of the forward and adjoint variables can be applied to assess the

change in model outcomes, uncertainities in flood impact and flood volume resulting from changes in control values and the individual uncertainties in each control variable. The adjoint sensitivity analysis is used here to establish relationships between certain controls and the system responses. A particular control problem is defined by selection of an appropriate objective function. This may require to be minimized in the case of data assimilation for example, or it may measure flood water levels in excess of some threshold as discussed in this paper. Once this objective function is defined, the adjoint sensitivity analysis is used to evaluate the gradient of this function with respect to the control variables or in other word the sensitivities. These in turn will be used to evaluate the uncertainty propagation through the model.

1. GOVERNING EQUATIONS FOR THE OPEN CHANNEL FLOW

The Saint Venant equations (SVE[s]) that take the effect of infiltration rate into consideration form a system of partial differential equations which represents mass and momentum conservation along the channel and include source terms for the bed slope and bed friction. These equations may be written as:

$$\frac{\partial A}{\partial t} + \frac{\partial Q}{\partial x} - f.b = 0 \tag{1}$$

$$\frac{\partial Q}{\partial t} + gA\left(\frac{\partial H}{\partial x} + \frac{\partial z}{\partial x}\right) + \frac{\partial(Qu)}{\partial x} + k\frac{Q|Q|}{A\,R} + \left(\frac{u.f}{2}\right).b = 0 \tag{2}$$

where t is time; x is the horizontal distance along the channel; Q is the discharge; A is the flow cross section area; H is the total water stage; g is the gravitational acceleration; z is the vertical distance between the horizontal datum and the channel bed as function (x,t); S_0 is the bed slope = $-\frac{\partial z}{\partial x}$; k is a friction factor = g/C^2 according to Chezy or = $gn^2/R^{(1/3)}$ according to Manning; and $\frac{\partial(Qu)}{\partial x}$ is the momentum flux term, or convective acceleration; b is the channel bottom width and f is the infiltration rate. The effect of infiltration rate is added to the (SVE[s]) using the Green - Ampt model (Green and Ampt, 1911) as follows:

$$f = \frac{dF}{dt} = -K\left(\psi_f + \frac{F}{\theta_s - \theta_i} - H\right)\frac{\theta_s - \theta_i}{F} \tag{3}$$

Where F is the cumulative depth of infiltration; K is saturated hydraulic conductivity; ψ_f is suction at the wetting front (negative pressure head); θ_i is initial moisture content; θ_s is saturated moisture content ; and H is the depth of ponding.

The estimation of the momentum loss due to seepage (u.f/2) used in the momentum equation (2) follows work by Abiola and Nikaloaos (1998). In simulating an unsteady channel flow during a flood wave event using the Saint Venant equations (SVE[s]), equation (1) and equation (2) are subjected to initial and boundary conditions. Initial conditions are Q(x,0) and A(x,0) and the boundary conditions are Q(0,t) and A(L,t) where x = L is the downstream limit of the model domain. Values Q(0,t) comprise the inflow hydrograph and A(L,t) are interpolated from within the domain using the method of characteristics (MOC), (Abbott, 1977) and (French, 1986) after modifying it to suit the case of channel flow over an infiltrating bed as described below, to provide a transparent downstream boundary through which the flood wave can pass without reflection.

2. ADJOINT SENSITIVITY ANALYSIS FOR SAINT VENANT EQUATIONS:

2.1. Defining the objective function

If the application of the analysis is to the control or assessment of risk of flood water levels then it is convenient to compare predicted levels with known threshold values above which flooding could occur. A quadratic measuring function, r, that quantifies the water depths greater than some specified threshold flood depth H_d, for which the corresponding threshold cross sectional area = A_d, may be defined as follows:

$$r = 0.25\{(A - A_d)^2 + |A - A_d|(A - A_d)\}\,\delta(x - x_o)\,\delta(t - t_o) \tag{4}$$

where A(x, t) is the flow cross section area calculated by the forward hydraulic model; and A_d (x_o, t_o) are threshold values at location $x = x_o$, and time $t = t_o$ based on the corresponding safe water level H_d.
Note that r = 0 for $A \leq A_d$ and r = 0.5 $(A - A_d)^2$ for $A > A_d$

2.2. Governing equation for the sensitivity analysis

Adjoint sensitivity analysis evaluates the sensitivities of the objective function to certain control variables. This is achieved by creating the Lagrangian and taking the first variation. The method follows closely that described by (Sanders and Katopodes, 1998), (Gejadze and Copeland, 2005), and (Elhanafy and Copeland, 2007a) as follows:

The cost function J is defined by integrating the weighted sum of the objective function and the residuals of the SVE[s] over the entire computational domain as follows:

$$J = \int_0^T \int_0^L \left\{ r + \phi\left[\frac{\partial A}{\partial t} + \frac{\partial Q}{\partial x} - f.b \right] + \psi\left[\frac{\partial Q}{\partial t} + gA\left(\frac{\partial H}{\partial x} + \frac{\partial z}{\partial x}\right) + \frac{\partial (Qu)}{\partial x} + k\frac{Q|Q|}{A R} + \left(\frac{u.f}{2}\right).b \right] \right\} dx\, dt \tag{5}$$

where; the weights φ and ψ are Lagrange multipliers later to be revealed as the adjoint variables and L and T are the spatial and temporal limits of the domain. The sensitivities and the adjoint equations are evaluated by taking the first variation of J in equation (5) with respect to all flow variables and control variables and using integration by parts. The final expression for the variation in J, δJ, is given by the sum of the following 6 integrals:-

$$
\begin{aligned}
\delta J \ =\ & \int_0^L \left[\phi\, \delta A + \psi\, \delta Q \right]_0^T dx + \int_0^T \left[\phi\, \delta Q + \psi\left(\frac{2Q}{A}\right)\delta Q - \psi\left(\frac{Q}{A}\right)^2 \delta A + \psi g H \delta A \right]_0^L dt \\[2mm]
& + \int_0^T \int_0^L \Bigg\{ \left[-\frac{\partial \phi}{\partial t} - gH\frac{\partial \psi}{\partial x} + \psi g\frac{\partial z}{\partial x} - \psi\, g\, n^2\, \frac{Q|Q|}{A^2 R^{(4/3)}} + \frac{Q^2}{A^2}\frac{\partial \psi}{\partial x} + \frac{\partial r}{\partial A} + \frac{\partial f}{\partial H}\left(\frac{\psi b}{2}\frac{Q}{A} - b\,\phi\right) - \frac{\psi b}{2}\frac{Q}{A^2}f \right]\delta A \\[2mm]
& + \left[-\frac{\partial \psi}{\partial t} - \frac{\partial \phi}{\partial x} + 2\,\psi\, g\, n^2\, \frac{|Q|}{A R^{(4/3)}} - 2\frac{Q}{A}\frac{\partial \psi}{\partial x} + \frac{\partial r}{\partial Q} + \frac{\psi}{2}\left(\frac{b f}{A}\right) \right]\delta Q \Bigg\} dx\, dt \\[2mm]
& + \int_0^T \int_0^L \left[\frac{u}{2}\psi - \phi \right] b\, \delta f\ dx\, dt + \int_0^T \int_0^L \left(2\,\psi\, g\, n\ \frac{Q|Q|}{A R^{(4/3)}} \right) \delta n\ dx\, dt - \int_0^T \int_0^L \left(g\,\psi\, A\right)\delta S_0\ dx\, dt
\end{aligned}
\tag{6}
$$

We are seeking variations in J that are caused by possible variations in Q and A as the initial conditions and at the upstream and downstream boundaries. We are also looking for the effects of variations in controls f, n, and S$_o$ in the domain. These are expressed by integrals 1, 2, 4, 5, and 6 respectively in equation (6). We are not looking for the effects of variations in Q and A within the domain as expressed by integral 3 in equation (6). Hence this integral is required to equal zero for any variations in Q and A. This conditions leads to the identification of the two adjoint equations from the kernal of this integral as follows:-

$$
\begin{aligned}
& \frac{\partial \phi}{\partial \tau} - gH\frac{\partial \psi}{\partial x} + \psi g\frac{\partial z}{\partial x} - \psi\, g\, n^2\, \frac{Q|Q|}{A^2 R^{(4/3)}} + \frac{Q^2}{A^2}\frac{\partial \psi}{\partial x} + \frac{\partial r}{\partial A} + \frac{\partial f}{\partial H}\left(\frac{\psi b}{2}\frac{Q}{A} - b\,\phi\right) - \frac{\psi b}{2}\frac{Q}{A^2}f = 0 \\[2mm]
& \frac{\partial \psi}{\partial \tau} - \frac{\partial \phi}{\partial x} + 2\,\psi\, g\, n^2\, \frac{|Q|}{A R^{(4/3)}} - 2\frac{Q}{A}\frac{\partial \psi}{\partial x} + \frac{\partial r}{\partial Q} + \frac{\psi}{2}\left(\frac{b f}{A}\right) = 0
\end{aligned}
\tag{7}
$$

Where $\tau = (T - t)$, measured in reverse time direction.

Solution of adjoint equations, equation (7), for given flow conditions Q and A ensures that integral 3 in equation (6) equals zero and provides values for φ and ψ everywhere in the domain. These values can be used in conditions derived from integrals 1, 2, 4, 5, and 6 in equation (6) to quantify the sensitivities as shown below.

2.3. Derivation of the sensitivities
2.3.1. Sensitivity to the upstream channel flow

Sensitivities to initial condtions are revealed by integral 1 in equation (6). If we impose the conditions φ (x,T) = ψ (x,T) = 0, that is no sensitivity information propagates into the domain at t = T, then the sensitivity to initial conditions is just $\dfrac{\delta J}{\delta A(x,0)} = -\phi$ and $\dfrac{\delta J}{\delta Q(x,0)} = -\psi$ at each discrete location along the channel. If we do not want to control the solution to any initial condition then we may set $\delta A(x,0) = \delta Q(x,0) = 0$ then integral 1 vanishes. Sensitivities to boundary conditions are revealed by integral 2 in equation (6). If we

impose the condition $\delta Q(L,t) = 0$, that is $Q(L,t)$ is not used as a control, then the sensitivity to inflow $Q(0,t)$ is shown to be :

$$\frac{\delta J}{\delta Q} = -\int_0^T \{\phi + 2\, u\, \psi\}dt \tag{8-a}$$

Or, by considering contribution to the local sensitivity of each point along the upstream boundary:

$$\frac{\delta J}{\delta Q(0,t_p)} = -\{\phi(0,t_p) + 2\,u(0,t_p)\,\psi(0,t_p)\} \tag{8-b}$$

at each time step or perturbation time from $t = 0$ to T.

Similarly by imposing condition $\delta A(0,t) = 0$, that is $A(0,t)$ is not used as a control, then the sensitivity to flow cross section area A is shown to be:

$$\frac{\delta J}{\delta A} = \int_0^T \{(gH - u^2)\psi\}dt \tag{9-a}$$

Or, by considering contribution to the local sensitivity of each point along the downstream boundary:

$$\frac{\delta J}{\delta A(L,t_p)} = \{g\,H(L,t_p) - (u^2)(L,t_p)\}\psi(L,t_p) \tag{9-b}$$

Figure (1) shows all of the required boundary conditions. We note that the boundary conditions for ψ $(0,t)$ and ϕ (L,t) are both required and must be defined such that both boundaries are transparent to the outgoing peturbations created within the adjoint domain. This is achieved by interpolation from available values within the domain using the method of characteristics (MOC); the formulation is given below.
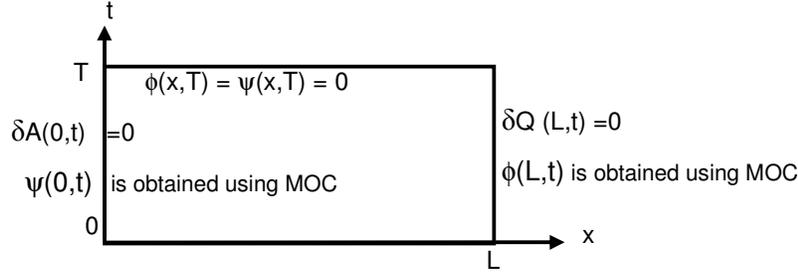
Figure (1). Boundaries and initial conditions for the solution domain

2.3.2. Sensitivities to spatially and temporary distributed variables

The sensitivities to bed slope, bed friction in terms of Manning's coefficient, and infiltration rate which are considered as control variables that affect the flood level at $x = x_0$ can be derived from equation (6). The sensitivity to bed slope is found from integral 6, $\dfrac{\delta J}{\delta S_0} = -\int_0^T \int_0^L g\,\psi\,A\,dx\,dt$ while the sensitivity to bed friction in terms of Manning's coefficient is found from integral 5, $\dfrac{\delta J}{\delta n} = \int_0^T \int_0^L \left(2\psi\,g\,n\,\dfrac{Q|Q|}{A\,R^{(4/3)}}\right)dx\,dt$ and the sensitivity to the infiltration rate is found from integral 4, $\dfrac{\delta J}{\delta f} = \int_0^T \int_0^L \left(\dfrac{u}{2}\psi - \phi\right)b\,dx\,dt$. These sensitivities can be evaluated after the two adjoint equations, equation (7) are solved for ϕ and ψ.

3. NUMERICAL APPROACH
3.1. Discretising the Forward Model

A simple space and time staggered finite difference mesh is used to discretise the domain as depicted in Figure (2). The approximation of the derivatives $\dfrac{\partial h}{\partial x}$ is $\left[\dfrac{h_i^j - h_{i-1}^j}{\Delta x}\right]$. A first order upwind scheme is used for the convective term $\dfrac{\partial(Qu)}{\partial x}$ which is discretised with two point upwind difference expression or a weighted average of centered and upwind difference expressions:

$$\frac{\partial (Qu)}{\partial x} = \frac{Qu(i+1) - Qu(i-1)}{2\Delta x} + \frac{0.5 \left(Qu(i-2) - 3Qu(i-1) + 3Qu(i) - Qu(i+1) \right)}{3\Delta x} \tag{10}$$

See (Fletcher, 1991), (Leonard, 1983) and (Falconer and Liu, 1988) for more details. The discharge Q is marched forward in time using the momentum equation (equation 2) as follow:

$$Q_i^{j+1} = Q_i^j - \left(\frac{gA_i^j}{Tw_i^j} \right)\left(\frac{\Delta t}{\Delta x} \right)\left[A_i^j - A_{i-1}^j \right] - gA_i^j \cdot \left(\frac{\Delta t}{\Delta x} \right)(z_i - z_{i-1}) - \Delta t \cdot g \, n^2 \cdot \frac{Q_i^j \left| Q_i^j \right|}{AR^{(4/3)}} - \Delta t \cdot \frac{\partial (Qu)}{\partial x} - \frac{\Delta t}{2} \cdot b_{i-1} \, f_i^j \, u_i^j \tag{11}$$

The flow cross section, A, is marched forward in time using the continuity equation (equation 1)

$$A_i^{j+1} = A_i^j \quad - \left(\frac{\Delta t}{\Delta x} \right)\left[Q_{i+1}^{j+1} - Q_i^{j+1} \right] + \Delta t \cdot b_{i-1} \, f_{i+1}^j \tag{12}$$

where; Tw is the channel top width, and b is the channel bottom width of a trapezoidal channel section. The initial conditions are A_i^1 and Q_i^1, while the boundary conditions are Q_1^{j+1} at the upstream boundary and A_{nx}^{j+1} at the downstream boundary, the upstream condition is the inflow hydrograph; the downstream condition must be interpolated using the method of characteristics (MOC) as described in Abbott [13] and French [14], see below.

The adjoint model which is represented by equation (7) is discretized using the same simple space and time staggered explicit finite difference scheme as illustrated in Figure (2).

3.2. Method of Characteristics (MOC):

Following a standard text such as (Abbott, 1977) and (French, 1986), the characteristics of the Saint Venant equations can be derived. The final form is:

$$\Delta Q + (-u \pm c)\Delta A + g \, n^2 \frac{Q|Q|}{AR^{(4/3)}} + gA \frac{\partial z}{\partial x} - (-u \pm c)f \, b + \frac{f \, u}{2}b = 0 \tag{13}$$

While characteristics of the adjoint model are identified as:

$$\Delta \phi + (u \pm c)\Delta \psi - 2\psi \, g \, n^2 \frac{Q|Q|}{A^2 R^{(4/3)}} + g\psi \frac{\partial z}{\partial x} + (u \pm c)(2\psi \, g \, n^2 \frac{|Q|}{A \, R^{(4/3)}}) = 0 \tag{14}$$

Where; Δ indicates a total change in the variable along the characteristic path. These formulas are used to interpolate boundary values of A, ϕ, and ψ.
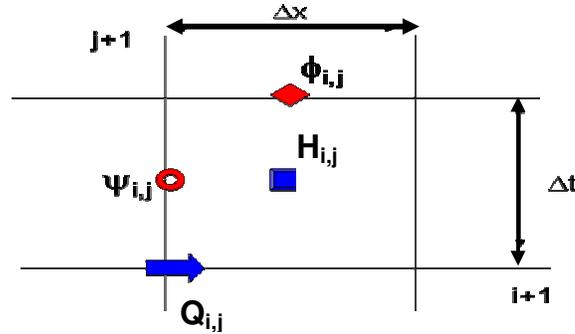
Figure (2). The discretization scheme for the forward and adjoint model

4. MODEL VERIFICATION
4.1. Forward model verification

Developing a complete test to check and validate an exact solution of the one dimensional Saint Venant equations is not possible. It is possible however to develop simple tests to compare the model results with analytical solutions of certain idealized cases. Several tests have been carried out to verify the model from uniform steady flow to non-uniform unsteady flow. The results showing the validity of the model have been reported elsewhere (Elhanafy and Copeland, 2007a) and (Elhanafy and Copeland, 2007b).

4.2. Adjoint verification

In the following experiment, a direct simulation is done first with a chosen boundary Q_1 and the computed results at certain location are considered to be the "observations" $Q_1(x = x_0)$ in a subsequent data assimilation. The model are re-run with a new boundary Q_2 and the results at same location were recorded

$Q_2(x = x_0)$. The discrepancy between the two solutions at $(x = x_0)$ is used to evaluate the measuring function, r. Then by using conjugate gradient minimization the resulting cost function, J is minimized at each iteration to recover Q_1 from Q_2. This technique where the same model is used to do the data assimilation and to produce the "observations" is called an identical twin experiment.
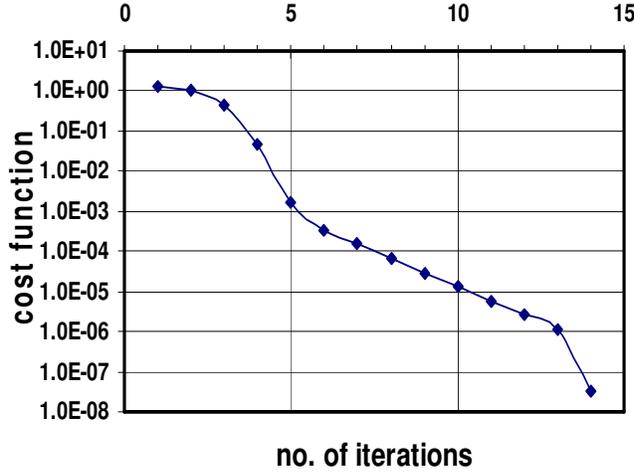
Figure (3). Cost function convergence
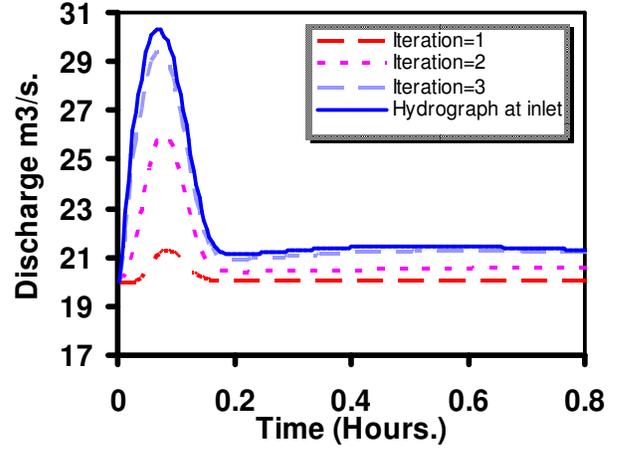
Figure (4). Recovering of Q1 from Q2 as a result of the identical twin experiment.

The convergence is rapid such that the inlet hydrograph, Q_1 is recovered after only 14 iterations, a reduction of the measuring function by a factor 100000 achieved in about 10 iterations and about 97 % of Q_1 is recovered after only three iterations as illustrated in Figure (3) and Figure (4).

5. EVALUATING THE UNCERTAINTIES FROM THE ADJOINT SENSITIVITIES:

To study the propagation of uncertainty in each of the control variables , a Gaussin pdf for each control variable is assumed to represent the uncertainty as illustrated in Figure (5). The overall uncertainty in the cost function, δJ, is then found from the expression:

$$\delta J = \left(\frac{\partial J}{\partial Q}\right)\delta Q + \left(\frac{\partial J}{\partial A}\right)\delta A + \left(\frac{\partial J}{\partial f}\right)\delta f + \left(\frac{\partial J}{\partial n}\right)\delta n + \left(\frac{\partial J}{\partial S_0}\right)\delta S_0 \tag{15}$$

where; $\dfrac{\partial J}{\partial Q}, \dfrac{\partial J}{\partial A}, \dfrac{\partial J}{\partial f}, \dfrac{\partial J}{\partial n}, and \dfrac{\partial J}{\partial S_0}$ are the sensitivities of the flood level at $x = x_0$ as described in section 2.3 with respect to the discharge upstream, the cross section of the water flow downstream, the infiltration rate, Manning coefficient, and the bed slope respectively, while $\delta Q, \delta A, \delta f, \delta n, and \delta S_0$ are the uncertainties of each of the control variables. Uncertainties represented by a Gaussian pdf are most conveniently expressed as a variance or covariance. Equation (15) can then be replaced by the following expression assuming no correlation between the control variables:

Figure (5). Gaussian distribution with zero mean and Unit variance

$$VarJ = \left(\frac{\partial J}{\partial Q}\right)^2 Cov(Q) + \left(\frac{\partial J}{\partial A}\right)^2 Cov(A) + \left(\frac{\partial J}{\partial f}\right)^2 Cov(f) + \left(\frac{\partial J}{\partial n}\right)^2 Cov(n) + \left(\frac{\partial J}{\partial S_0}\right)^2 Cov(S_0) \tag{16}$$

Equation (16) provides a way to compute the combined uncertainty in (J) from the uncertainties in its component parts. When considering the discretised model we should use the matrix formulation. For example, if we have uncertainty in one control variable n then the total variance in the objective function J due to the covariance of n is given by:

6

$$VarJ = \left[\frac{\partial J}{\partial n}\right]^{T} \left[Cov\,(n)\right]\left[\frac{\partial J}{\partial n}\right]$$

(17)

where; $\left[\frac{\partial J}{\partial n}\right] = 2\psi\,g\,n\,\frac{Q|Q|}{A\,R^{(4/3)}}$, is the vector of local sensitivities computed in each cell. As engineers

we need a physical interpretation of the objective function J and its variance Var J. We can interpret the

objective function, $J = \iint r\,dx\,dt = \iint 0.5\,(A - A_d)^2\,\delta(x - x_0)\,\delta(t - t_0)\,dx\,dt$, with units (m^{5}s), as a

measure of flood impact. Also, since r = 0 for A ≤ A$_d$ and r = 0.5 (A - A$_d$)^2 for A > A$_d$, we can scale J by the

mean flood excess cross sectional area $I = \frac{0.25}{L\,T}\iint\{(A - A_d) + |A - A_d|\}\delta(x - x_0)\,\delta(t - t_0)\,dx\,dt$. Now

we can define the flood impact, $P = \frac{J}{I}$ (m^3.s) and $Var\,(P) = \frac{Var\,(J)}{I^2}$ (m^3.s)^2 which have more convenient

units. However, we are more likely to be interested in the flood impact in a particular reach rather than over
the whole domain. So, it is useful to note that we are free to decide in which part of the model domain we
wish to evaluate the flood impact. If, for example, we are interested in the flood impact for a reach of length
ΔL$_f$ and for duration of the flood event ΔT_f as shown in Figure (11), then these length and time scales can be
used to scale J and I. This achieved by controlling the non-zero part of the kernel of the integrals that

define J and I by means of the kronecker delta function $\delta\,(x - x_o)\,\delta\,(t - t_o)$ where locations $x_0 \in \Delta\,L_f$ and

times $t_0 \in \Delta\,T_f$.

6. REAL CASE STUDY:
6.1. Location and stream geometry:
A case study was applied to the main stream of El-Daba watershed at the north coast of Egypt. The
watershed area is about 51km^2, and the main stream runs about 15 km from the outlet station of the
watershed. From field measurements (Elhanafy at al, 1999), it is found that the channel cross section is
trapezoidal with 14 m. average bottom width and (1:1) side slope as shown in Figure (6). Flow in the channel
is simulated for a period of 40 minute during which time a sinusoidal hydrograph shape of duration 13 minute
as shown in Figure (7) introduced at the upstream boundary, passes along the channel to represent a flash
flood event. The peak discharge is 9.4 m^3.s^{-1}.

| Figure (6) Channel cross section | Figure (7) A flash flood hydrograph at the upstream boundary. |
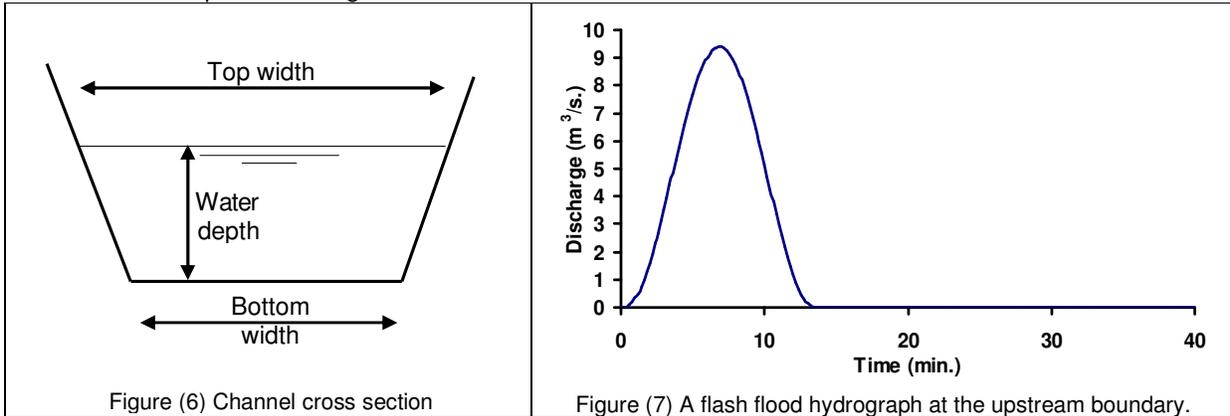
6.2. Parameter identification:
Although the channel length is 15 km, we study only the upstream reach of length 6 km. This is

because the measuring stations $x_0 \in \Delta\,L_f$ are located 3 km from the upstream boundary as discussed in

section (6.4). In this reach, Manning friction coefficient is found to be 0.016 m$^{-1/3}$.s ref (Elhanafy at al, 1999)
this characterises a straight, clean, non-erodable earth channel. The bed slope of the main stream is found
to be (2.7%) along the whole channel. The infiltration rate is a function of the saturated hydraulic
conductivity, the suction at the wetting front, the initial moisture content, and the saturated moisture content.

The values in Table (1) are chosen for these variables based on previous studies (Elhanafy at al, 1999) to calculate the infiltration rate from equation (3).

saturated hydraulic conductivity	k	1.0 E-5	(m/s)
suction at wetting front	ψ_f	-0.10	(m.)
initial moisture content	θ_i	0.318	(dimensionless)
saturated moisture content	θ_s	0.518	(dimensionless)

Table (1) Infiltration parameters

6.3. Defining parameter uncertainties:

We assume that the variance of each control variable is uniform along the channel and has the values given in Table (2). These values represent the uncertainty in each control variable. The variance in Manning coefficient n follows Guganesharajah et al (2006), and represents an uncertainty in n of approximately 20%. The variance in S_0 represents an uncertainty in the bed slope of approximately 1%. The variance in the infiltration rate, f, which is spatially and temporarily variable and difficult to measure, represents an uncertainty of 50%. The variance of the upstream discharge is assumed to be proportional to the upstream discharge Q such that Var(Q)= $0.001Q^2$ as shown in Figure (8). The correlation function for each control variable is illustrated in Figure (9), from which the covariance at each control variable is calculated as follows: $Co\,\mathrm{var}\,(control\quad \mathrm{var}iable\,) = r * Var\,(control\quad \mathrm{var}iable\,)$ (18)

where: r, is the correlation function shown in Figure (9).

Var (f)	1.0 E -10	$(m/s)^2$
Var (S_0)	1.0 E -7	(dimensionless)
Var (n)	1.0 E -5	$(m^{(-1/3)}.s\,)^2$

Table (2) Variances of Control variables.
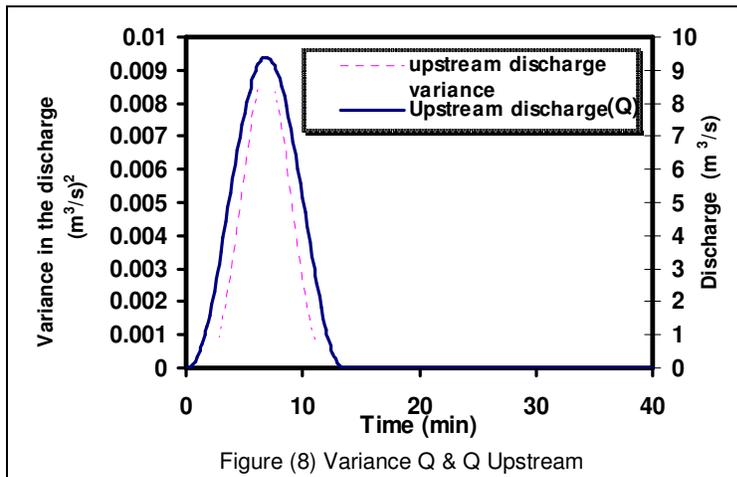
Figure (8) Variance Q & Q Upstream
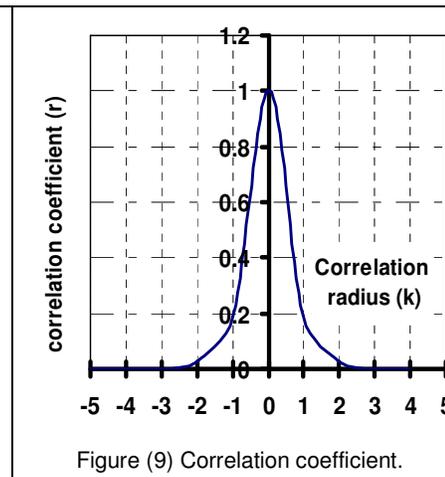
Figure (9) Correlation coefficient.

6.4. Defining the flood event and flood impact:

The flood wave is illustrated in Figure (10) which shows water depths plotted against time and distance along the channel. The effect of the inflow hydrograph at x = 0 is clearly shown from 0 to 13 minutes. While the effect of channel storage is evident up to t = 40 minutes. The wave propagates and decays with distance along the channel. The leading characteristic (leading edge of wave front) is shown by the arrow. The measuring locations $x_0 \in \Delta L_f$ are chosen to be near a culvert, located 3 km from the upstream boundary, which lies beneath the international coastal highway which extends from Egypt to Libya. A threshold cross sectional area A_d = 5.0 m^2 is chosen at x_0 = 3.0 km with ΔL_f = 1.0 m. This represent a threshold water level of 0.26 m. A small value such as this indicates only the presence of the flood wave rather than a significant risk of damage or danger. Once the forward model has been integrated as shown in Figure (10),

8

the value of the objective function, J, evaluated from equation (5) and based on the measuring function r defined in equation (4), is found to be 322.4 (m^5.s), while the scaling function I is found to be 0.34 (m^2). The flood duration ΔT_f, i.e. when A > A_d is found to be 19.8 minutes as shown in Figure (11). Consequently the flood impact, P, is calculated to be equal to 952.4 (m^3.s). This is equivalent to a mean excess wetted cross sectional area (i.e. wetted cross sectional area greater than A_d = 5.0 m^2) equal to

$$\frac{952.4}{\left(\Delta T_f\right)\left(\Delta L_f\right)} = 0.8 \; m^2 .$$
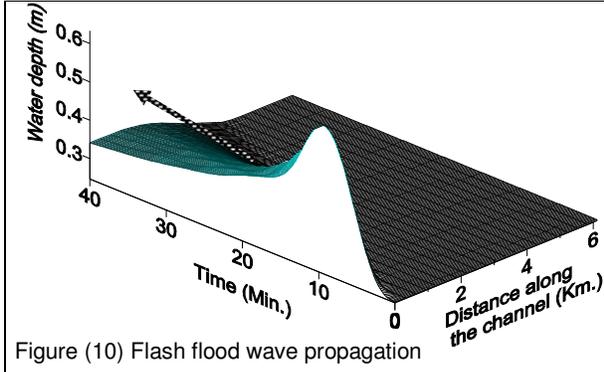
Figure (10) Flash flood wave propagation
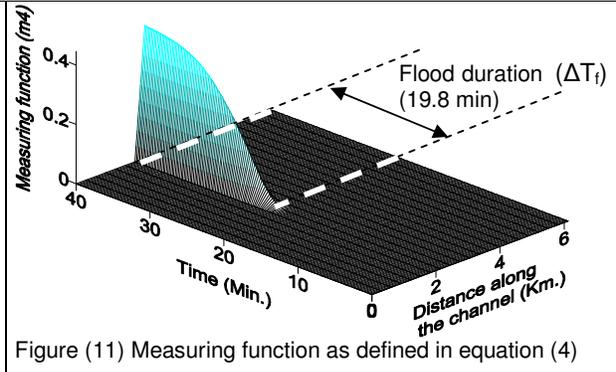
Figure (11) Measuring function as defined in equation (4)

6.5. Adjoint sensitivity:

The adjoint equations (7) are solved backward in time so evaluating the adjoint variables [φ, ψ] across the whole domain. These values are then used to quantify the sensitivities defined in Section 2.3. Sensitivity information propagates backward in time and space away from the flood location (ΔL_f and ΔT_f) toward the upstream boundary. The information about $\frac{\partial J}{\partial S_0}, \frac{\partial J}{\partial n}$ and $\frac{\partial J}{\partial f}$, representing the sensitivities of the flood impact to the bed slope, bed friction, and infiltration rate, are shown in Figures (12, 13, and 14) respectively, while the information about $\frac{\partial J}{\partial Q}$ captured at x = 0 is shown in Figure (15).
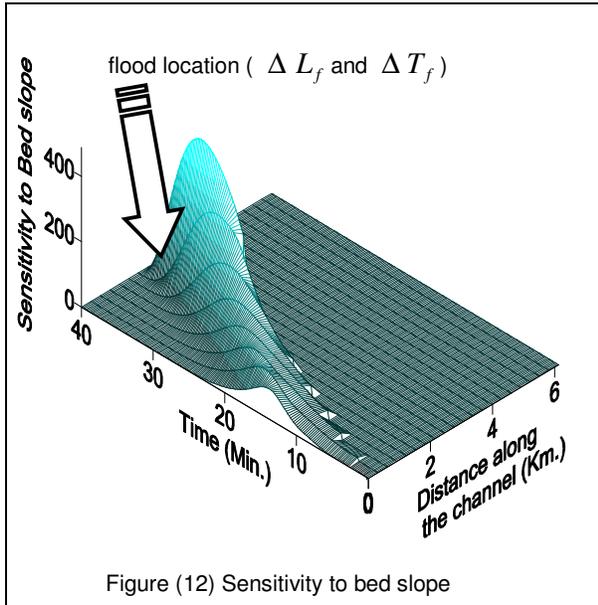
Figure (12) Sensitivity to bed slope
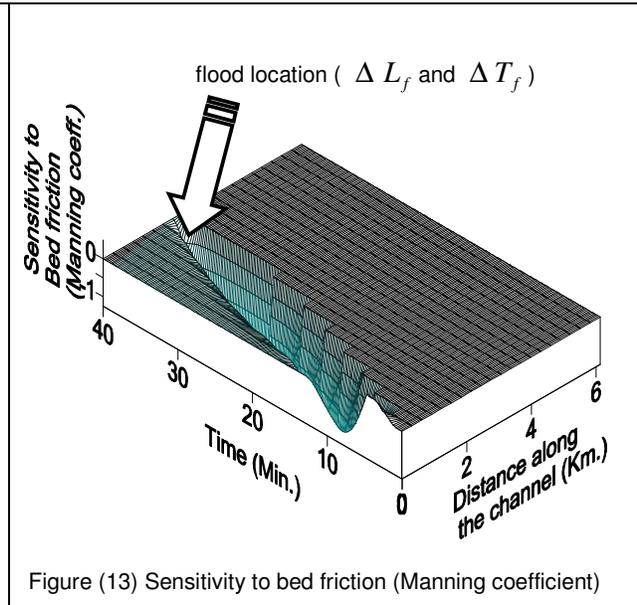
Figure (13) Sensitivity to bed friction (Manning coefficient)
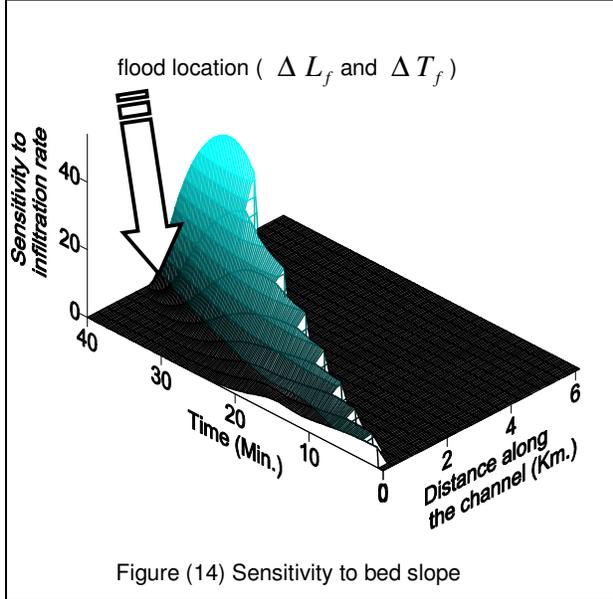
Figure (14) Sensitivity to bed slope
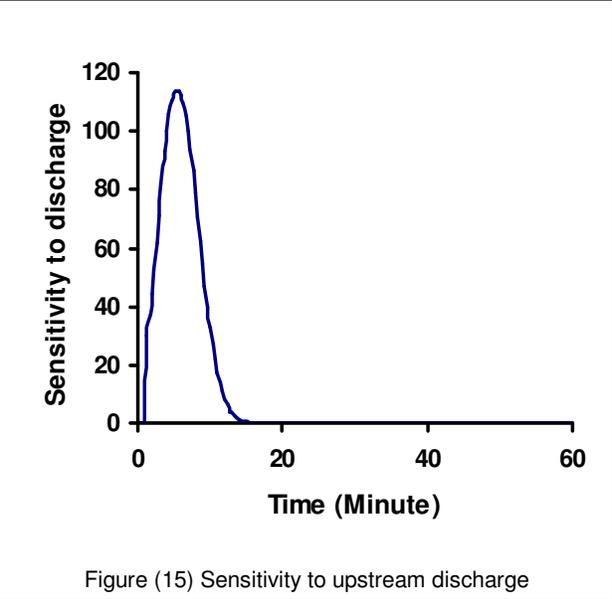
Figure (15) Sensitivity to upstream discharge

6.6. Uncertainties:

We have evaluated the total flood impact, P, that arises from a water depth excess above H_d within ΔL_f and ΔT_f. We now need estimates of the uncertainty in this flood impact. This is evaluated through the variance in the objective function J, Var (J) and the variance in the flood impact Var (P). Furthermore we can also represent uncertainty by the standard deviation of the flood impact, $\sigma_P = \{$Var (P)$\}^{1/2}$, and by a percentage uncertainty in the flood impact (σ_P/P)x100 %. Values for these measures of uncertainty for each control variable are given in Table (3). These results, based on plausible levels of uncertainty in each control variable, indicate that the predicted flood impact is most sensitive to the upstream discharge and least sensitive to the infiltration rate and that the overall percentage uncertainty in the flood impact is about 23%. These results demonstrate both the ranking of controls in any given flood event and the combined predictive uncertainties.

	Variance in J $(m^5.s)^2$	Variance in the flood impact $(m^3.s)^2$	Standard deviation in the flood impact $(m^3.s)$	% of error in the flood impact
due to (S_0)	44.4	388	19.7	6.11
due to (n)	0.60	5.25	2.29	0.71
due to (infiltration)	6.15E-4	5.36E-3	7.33E-2	0.0227
due to (upstream discharge)	294	2654	50.5	15.7
Total	339	3047	74.5	22.5%

Table (3) Measures of uncertainty in the flood impact due to the uncertainty in the control variables

7. CONCLUSIONS:

The adjoint method is applied to find the sensitivity of flood impact to uncertainties in some control variables. A flood event is simulated by solving the Saint Venant equations and sensitivity information found from the solution of the adjoint equations. This allows the overall uncertainty in flood impact to be calculated in a single model run. This much more efficient than the conventional methods based on ensemble techniques and reveals much more about the propagation of uncertainty through the model domain.

ACKNOWLEDGMENTS

REFERENCES

Abbott M.B. (1977), An Introduction to the method of characteristics, Thames and Hudson,London UK.

Abiola, A.A. and Nikaloaos, D.K. (1988), Model for flood propagation on initially dry land. ASCE Journal of Hydraulic Engineering, vol 114, No. 7, pp 689-707.

Cacuci, D.G. (2003), Sensitivity and uncertainty analysis, Volume I, Chapman & Hall CRC.

Copeland, G.J.M. & El-Hanafy, H. (2006), Computer modelling of channel flow using an inverse method, Proc. 6th Int. Conf. on Civil and Arch. Eng, Cairo.

Ding, Y. and Wang, S.Y. (2006), Optimal control of open channel flow using adjoint sensitivity analysis, Journal of Hydraulic Engineering, ASCE, vol. 132, no. 11, pp 1215-1228

Ding, Y., Jia Y., and Wang, S.Y. (2004), Identification of Manning's roughness coefficients in shallow water flows, Journal of Hydraulic Engineering, ASCE, vol. 130, no. 6.

El-Hanafy, H. and Copeland, G.J.M., (2007a). 'Mitigation of flash floods in arid regions using adjoint sensitivity analysis', Proc. of 11th IWTC Conf. 15-18 March, 2007, Sharm El-sheikh, Egypt

El-Hanafy, H. and Copeland, G.J.M., (2007b). 'Flood risk assessment using adjoint sensitivity analysis', Proc. of Proceedings of 32nd IAHR Congress 1-6 july, 2007, Venice, Italy

EL-Hanafy, H.M., Abdelmetaal, N.H., Elmongy, A.E. and Moussa, O. M, (1999), ' Protection of The Northern coast international highway at Wadi EL-Graola against flash floods. Proc. 6th Int. Conf. on Civil and Arch. Eng, Cairo, March 1999.

Falconer, R.A. and Liu, S.Q. (1988), Modeling solute transport using QUICK scheme, ASCE Journal of Environmental Engineering, vol. 114, pp. 3-20.

Fletcher, C.J. (1991), Computational techniques for fluid dynamics 1: Fundamental and General Techniques, Springer-Verlang.

French, R.H. (1986), Open Channel Hydraulics, McGraw Hill.

Gejadze, I. Yu and Copeland, G.J.M., (2005) 'Open boundary control for Navier-Stokes equations including the free Surface: adjoint sensitivity analysis', Computers & Mathematics with Applications, Elsevier.(accepted for publication)

Gejadze, I.Yu and Copeland, G.J.M. (2005), Adjoint sensitivity analysis for fluid flow with free surface, Int. J. Numer. Methods in Fluids, vol 47, Issue 8-9,pp 1027-1034.

Guganesharajah, K., Lyons, D.J., Parsons S.B. and Lioyd B.J. (2006), Influence of uncertainties in the estimation procedure of flood water level. ASCE Journal of Hydraulic Engineering, vol 132, No. 10, pp 1052-1060.

Leonard, B.P. (1983), Third-Order upwinding as a rational basis for computational fluid dynamics, Computational Techniques & Applications: CTAC-83, Edited by Noye, J. And Fletcher, C., Elsevier.

Moussa, O.M., Abdelmetaal, N.H., Elmongy, A.E, .and EL-Hanafy, H.M., (1999), Effect of environmental changes on drainage patterns and urban planning along coastal regions (case study), Proceedings of third International Conference On Civil & Architecture Engineering, Military Technical College, Kobry Elkobbah, Cairo Egypt, pp. 1-17, SU9.

Navon, I.M. and Zou, X. (1991), Application of the adjoint model in meteorology, Proceedings of the International Conference on Automatic Differentiation of Algorithms: Theory, Implementation and Application, SIAM Publications, A. Griewanek and G. Corliss Eds, SIAM, Philadelphia, PA .

Sanders, B.F and Katopodes, N.D. (1998), Control of multi-dimensional wave motion in shallow-water, Proceedings of the 5th Int. Conf. on Estuarine and Coast. Modeling, M. L. Spaulding, ed. pp. 267-278

Sanders, B.F and Katopodes, N.D. (2000), Adjoint sensitivity analysis for shallow-water wave control, Journal of Engineering Mechanics, ASCE, vol. 126, no. 9, pp 909-919

W.H. Green and G.A. Ampt, 'Studies on soil physics. Part I. The flow of air and water through soils', J. Agric. Sci., 4, 1–24 (1911).